Supporting Information (SI)

Thermotropic chirality enhancement of nanoparticles constructed from foldamer/bis(amino acid) complexes

Yuan Qiu,‡[a] Shuang Cao,‡[a] Chenchen Sun,[a] Qian Jiang,[a] Chongmo Xie,[a] Hong Wang,[a] Yonggui Liao,*[ab] Xiaolin Xie[b]

[a]Key Laboratory of Material Chemistry for Energy Conversion and Storage, Ministry of Education, Hubei Key Laboratory of Materials Chemistry and Service Failure, School of Chemistry and Chemical Engineering, Huazhong University of Science and Technology, Wuhan 430074, China

[b]National Anti-counterfeit Engineering Research Center, Huazhong University of Science and Technology, Wuhan 430074, China

‡These authors contribute equally to this work.

*Corresponding author.

Prof. Yonggui Liao, +86-27-8754-0053 (Tel), +86-27-8754-3632 (Fax), E-mail: ygliao@mail.hust.edu.cn

Experimental section

Materials

L-Homocystine and L-cystine were purchased from Energy Chemical Technology Co., Ltd. Chloroform and acetonitrile were available from Sinopharm Chemical Reagent Co., Ltd.

Characterization

Circular dichroism (CD) and ultraviolet-visible (UV−Vis) absorption spectra were taken on a JASCO J-810 spectropolarimeter. The fluorescence spectra were measured on a JASCO FP-6500 spectrofluorescence. Transmission electron microscopy (TEM) images were recorded using a FEI Talos F200X with an acceleration voltage of 200 kV. The samples for TEM observation were prepared by dropping the solution onto a carbon-coated copper grid and dried under vacuum at room temperature for 6 h.

Synthesis of **L-Hcy**

L-Homocystine (5.0 g, 18.6 mmol) was added to methanol (100 mL) at 0 ℃. After stirring for 10 min, a 70% water solution of perchloric acid (5.35 g, 37.3 mmol) was then added to the solution. The resultant mixture was stirred at room temperature overnight and the solvent was concentrated under reduced pressure. The residue was purified by recrystallization from acetonitrile/chloroform (1/19, v/v) to afford **L-Hcy** as a colorless crystalline solid (3.19 g, 37%). ^{1}H NMR (400 MHz, DMSO-d_6, TMS, ppm): δ = 8.27 (s, -CH-N$\boldsymbol{H}_3^+$, 3H), 4.01 (q, J = 5.2 Hz, -C$\boldsymbol{H}$-NH$_3^+$, 1H), 2.88–2.76 (m, -S-C$\boldsymbol{H}_2$-, 2H), 2.24–2.07 (m, -C$\boldsymbol{H}_2$-CH-, 2H). ^{13}C NMR (100 MHz, DMSO-d_6, TMS, ppm): δ = 171.1 (-$\boldsymbol{C}$OOH), 51.3 (-$\boldsymbol{C}$H-NH$_3^+$), 32.8 (-$\boldsymbol{C}$H$_2$-CH-), 30.0 (-S-$\boldsymbol{C}$H$_2$-).

Synthesis of ***L*-Cys**

The synthesis of **L-Cys** was conducted in the same way as that of **L-Hcy**. Yield: 42%. Spectroscopic data of **L-Cys**. ^{1}H NMR (400 MHz, DMSO-d_6, TMS, ppm): δ = 8.75 (s, -CH-N***H***$_3^+$, 3H), 4.21 (t, J = 8.0 Hz, -C***H***-NH$_3^+$, 1H), 3.39–3.29 (m, -S-C***H***$_2$-, 2H). ^{13}C NMR (100 MHz, DMSO-d_6, TMS, ppm): δ = 169.7 (-***C***OOH), 51.7 (-***C***H-NH$_3^+$), 37.8 (-S-***C***H$_2$-).

CD, UV−Vis absorption and fluorescence measurements

In the CD, UV–Vis absorption and fluorescence titrations of **Poly-1** with **L-Hcy** and **L-Cys**, stock solutions of **Poly-1** (2.4 mM) in chloroform and **L-Hcy** and **L-Cys** (48 mM) in acetonitrile were prepared. To 5 mL vessels equipped with a screwcap were added the stock solutions of **L-Hcy** or **L-Cys** (12.5, 25, 50, 62.5, 75, 87.5, 100, 150, 200, 250, 300, 350, 400, and 450 μL), respectively. A 50 μL of the stock solution of **Poly-1** was transferred to the vessels, and the resulting solutions were diluted with acetonitrile to keep the **Poly-1** concentration at 240 μM. CD, UV–Vis absorption and fluorescence spectra were then measured in the 1 mm quartz cell. The concentration of **Poly-1** was calculated on basis of the monomer units.

Supporting data

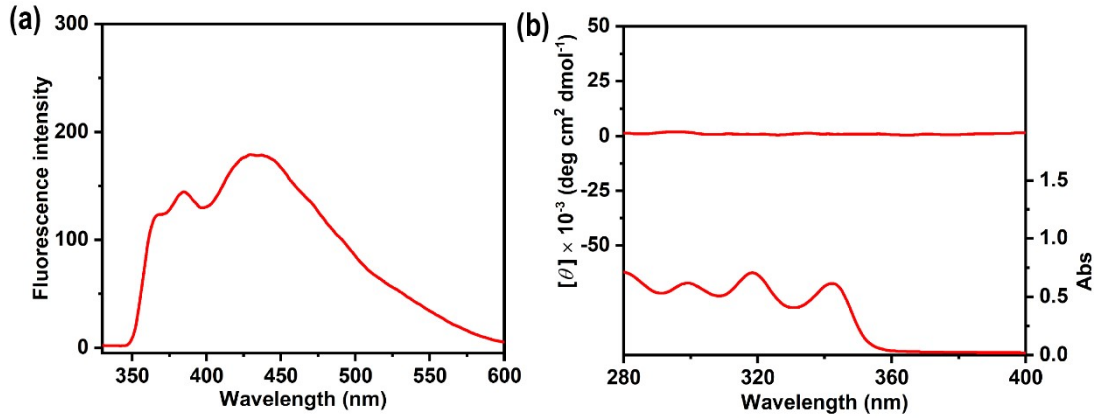

Fig. S1. (a) Fluorescence (λ_{ex} = 310 nm), (b) CD (top) and UV–Vis absorption (bottom) spectra of **Poly-1** in $CHCl_3/CH_3CN$ (1/9, v/v) at room temperature. [**Poly-1**] = 240 μM.

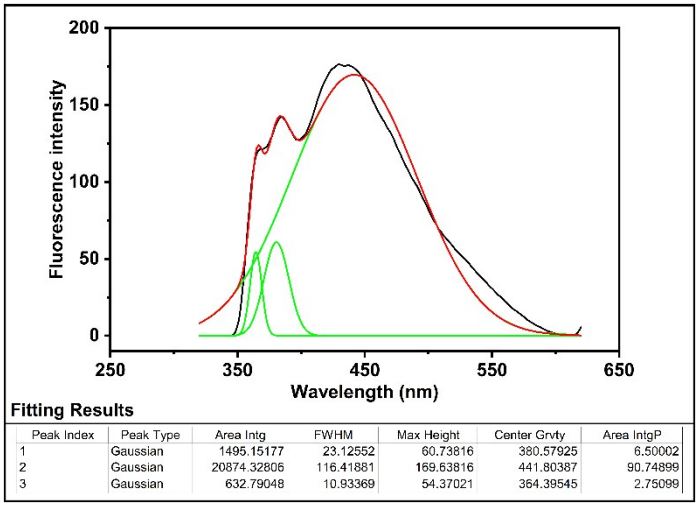

Peak Index	Peak Type	Area Intg	FWHM	Max Height	Center Grvty	Area IntgP
1	Gaussian	1495.15177	23.12552	60.73816	380.57925	6.50002
2	Gaussian	20874.32806	116.41881	169.63816	441.80387	90.74899
3	Gaussian	632.79048	10.93369	54.37021	364.39545	2.75099

Fig. S2. Peak-differentiation-imitating analysis of fluorescence spectrum for pure **Poly-1**.

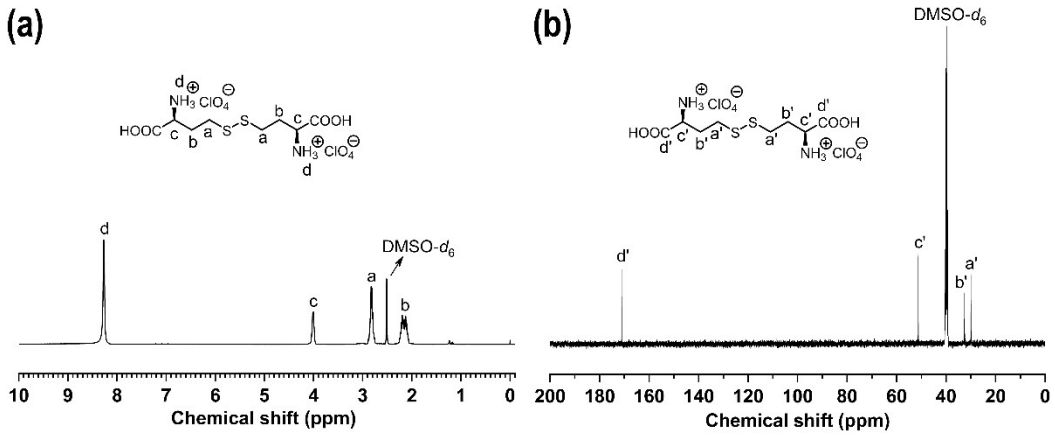

Fig. S3. ^1H (a) and ^{13}C NMR (b) spectra of **L-Hcy** in DMSO-d_6 at room temperature.

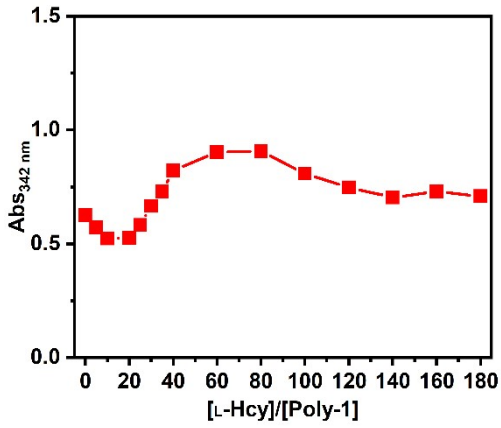

Fig. S4. Plot of absorbance at 342 nm for **Poly-1** versus the concentration ratio of L-**Hcy** to **Poly-1**.

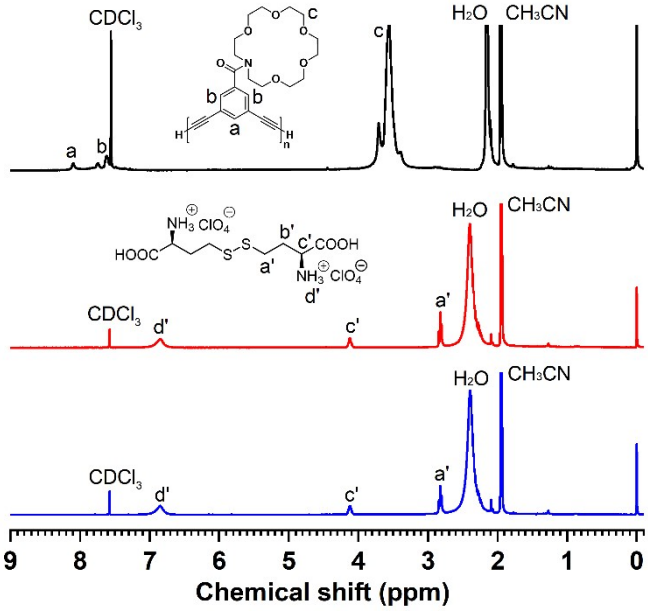

Fig. S5. ^{1}H NMR spectra of **Poly-1** (a), L-**Hcy** (b), and **Poly-1** with 10 equiv L-**Hcy** (c) in $CDCl_3/CD_3CN$ (1/9, v/v) at room temperature. [**Poly-1**] = 240 μM; [**L-Leu**] = 2.4 mM.

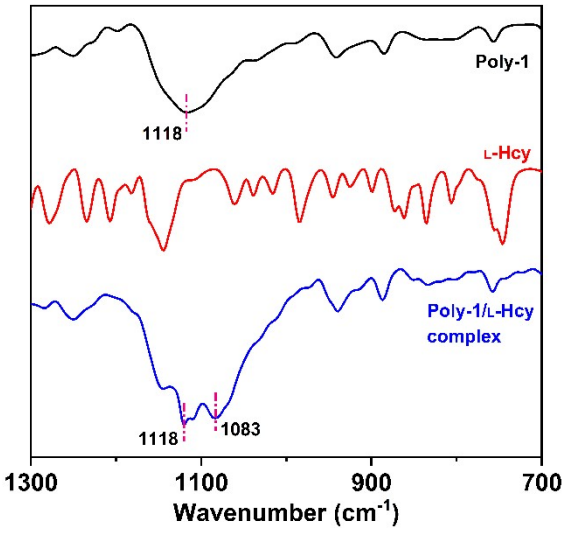

Fig. S6. FT-IR spectra of **Poly-1** (top), L-**Hcy** (middle), and **Poly-1** with 10 equiv L-**Hcy** (bottom) measured at room temperature (KBr tablet).

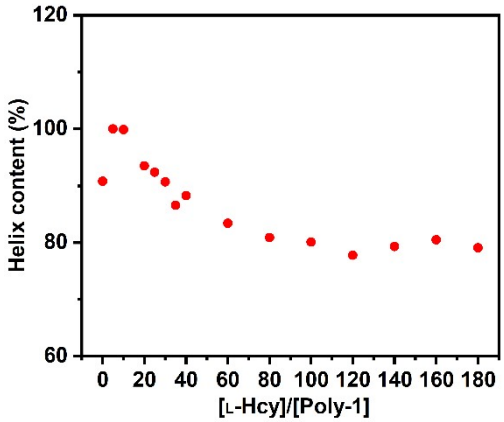

Fig. S7. Plot of helix content for **Poly-1** versus the concentration ratio of L-**Hcy** to **Poly-1**.

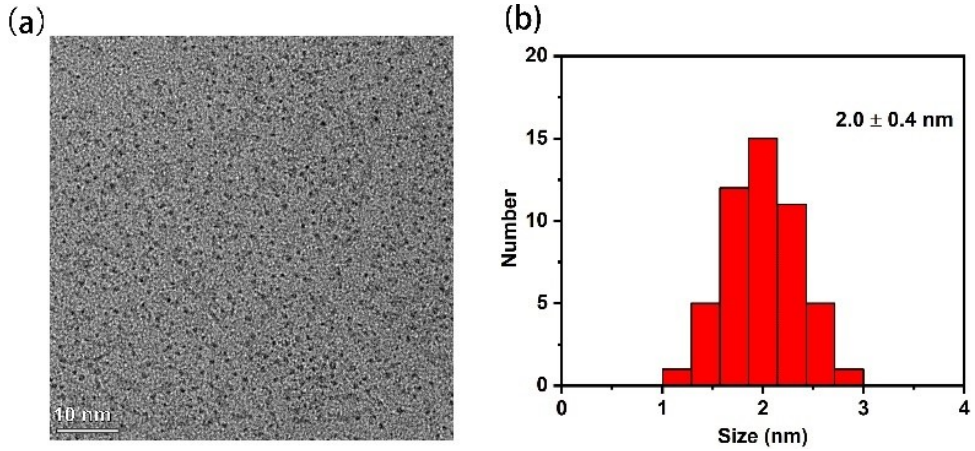

Fig. S8. (a) TEM image and (b) the corresponding histogram of particle size distribution of pure **Poly-1** in $CHCl_3/CH_3CN$ (1/9, v/v) at room temperature. [**Poly-1**] = 240 μM.

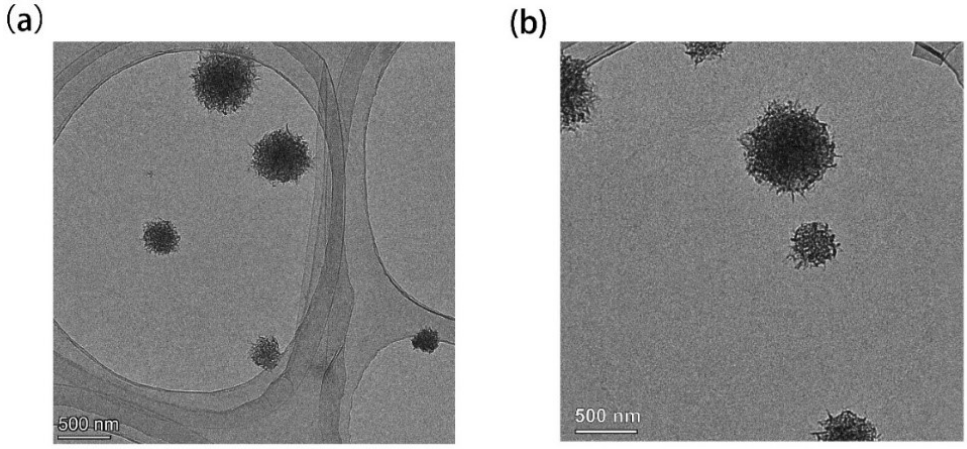

Fig. S9. TEM images of the mixtures between **Poly-1** and L-**Hcy** at a [L-**Hcy**]/[**Poly-1**] ratio of 40/1 (a) and 60/1 (b) in $CHCl_3/CH_3CN$ (1/9, v/v) at room temperature. [**Poly-1**] = 240 μM.

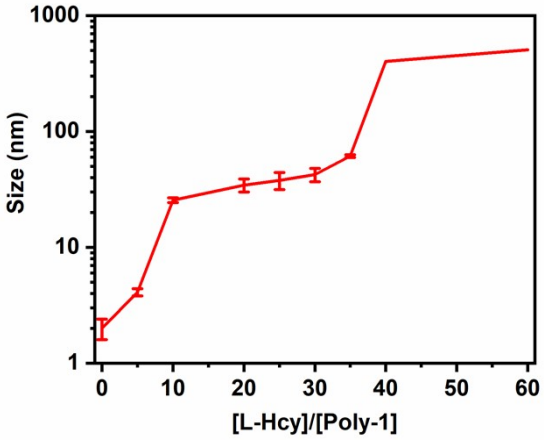

Fig. S10. Plot of average particle size of chiral **Poly-1**/L-**Hcy** nanoparticles versus the concentration ratio of L-**Hcy** to **Poly-1**.

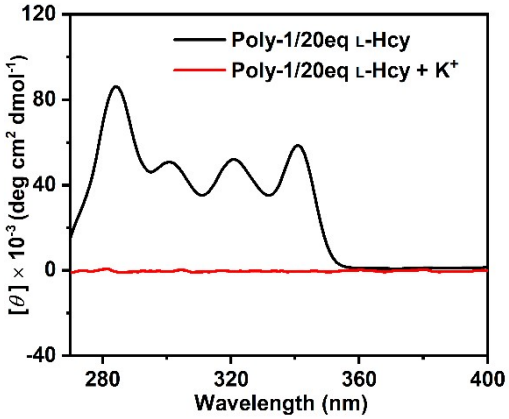

Fig. S11. CD spectrum of **Poly-1** complexed with 20 equiv L-**Hcy** before and after the addition of K^+ in $CHCl_3/CH_3CN$ (1/9, v/v) at room temperature. [**Poly-1**] = 240 μM.

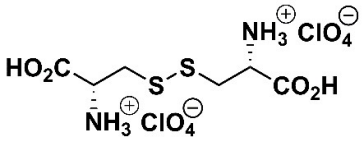

L-**Cys**

Scheme S1. Chemical structure of L-**Cys**.

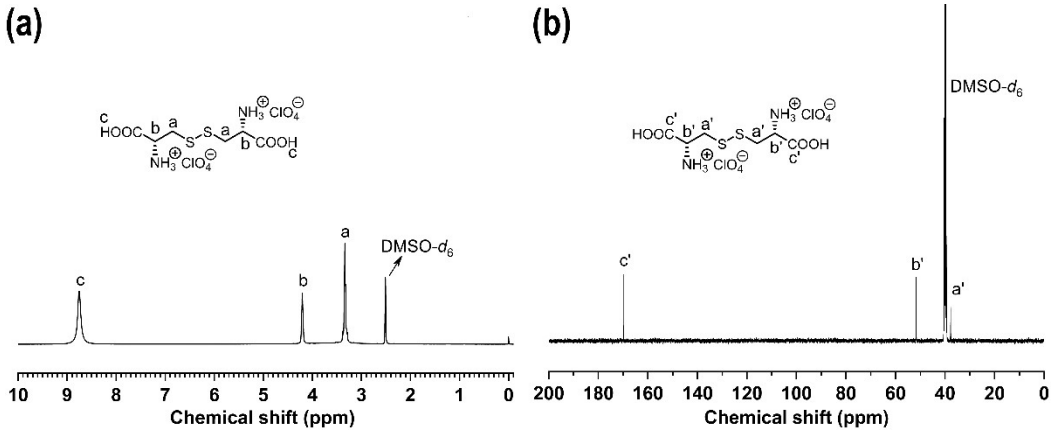

Fig. S12. ^1H (a) and ^{13}C NMR (b) spectra of L-**Cys** in DMSO-d_6 at room temperature.

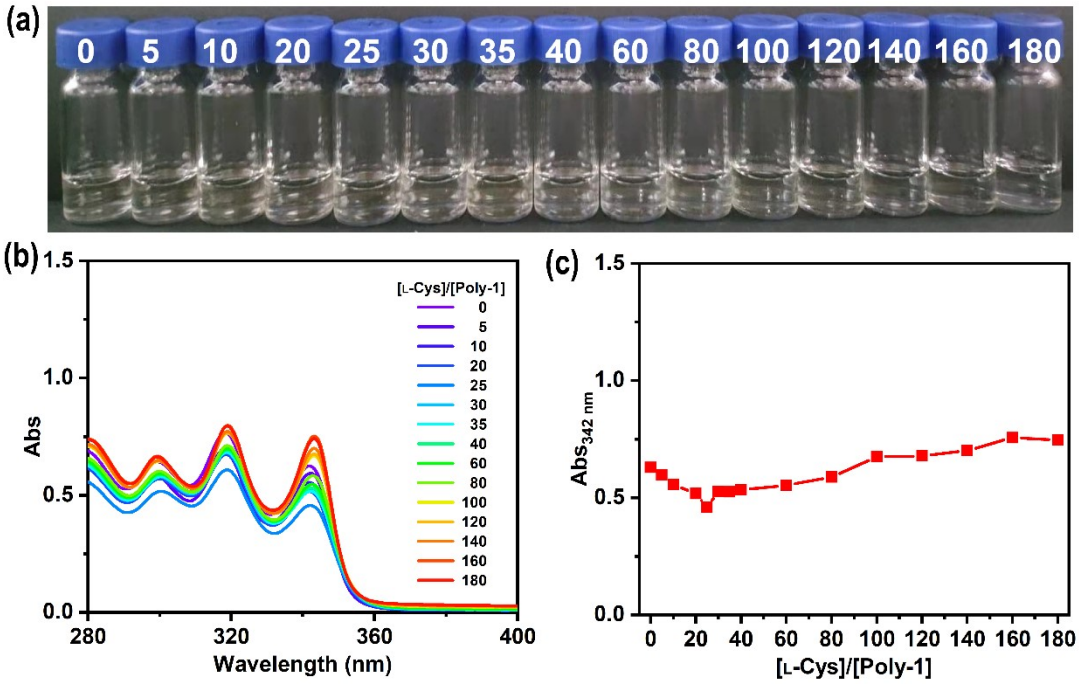

Fig. S13. Photographs (a) and UV–Vis absorption spectra (b) of **Poly-1** in the presence of L-**Cys** in $CHCl_3/CH_3CN$ (1/9, v/v) at room temperature. [**Poly-1**] = 240 μM. (c) Plot of absorbance at 342 nm for **Poly-1** versus the concentration ratio of L-**Cys** to **Poly-1**.

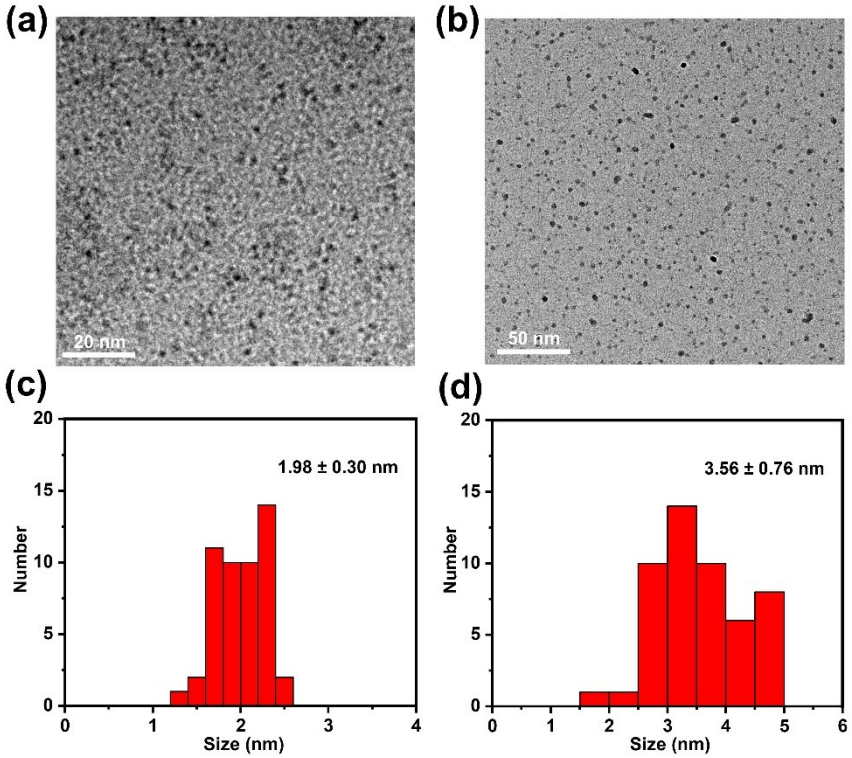

Fig. S14. TEM images and the corresponding histograms of particle size distribution of the mixtures between **Poly-1** and L-**Cys** at a [L-**Cys**]/[**Poly-1**] ratio of 35/1 (a, c) and 180/1 (b, d) in $CHCl_3/CH_3CN$ (1/9, v/v) at room temperature. [**Poly-1**] = 240 μM.

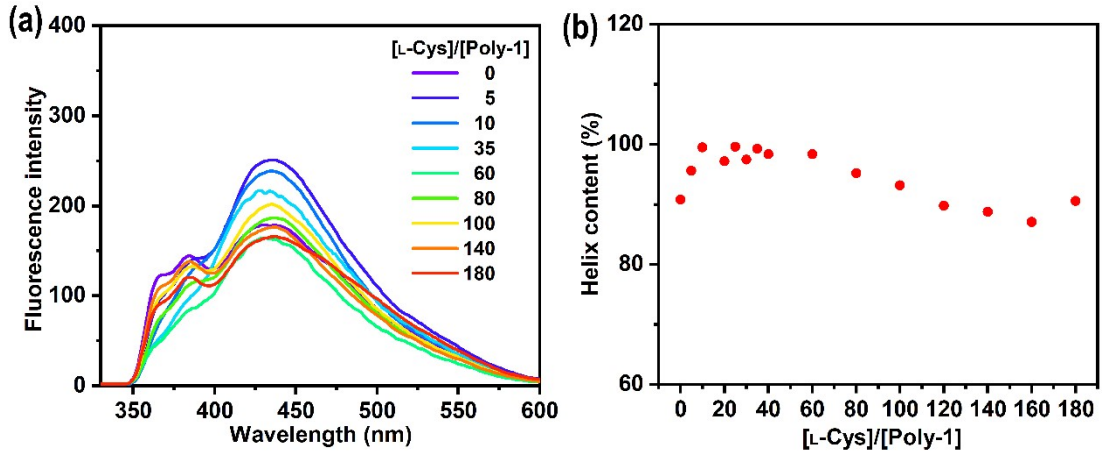

Fig. S15. (a) Fluorescence spectra of **Poly-1** in the presence of L-**Cys** in $CHCl_3/CH_3CN$ (1/9, v/v) at room temperature. [**Poly-1**] = 240 μM; λ_{ex} = 310 nm. (b) Plot of helix content for **Poly-1** versus the concentration ratio of L-**Cys** to **Poly-1**.

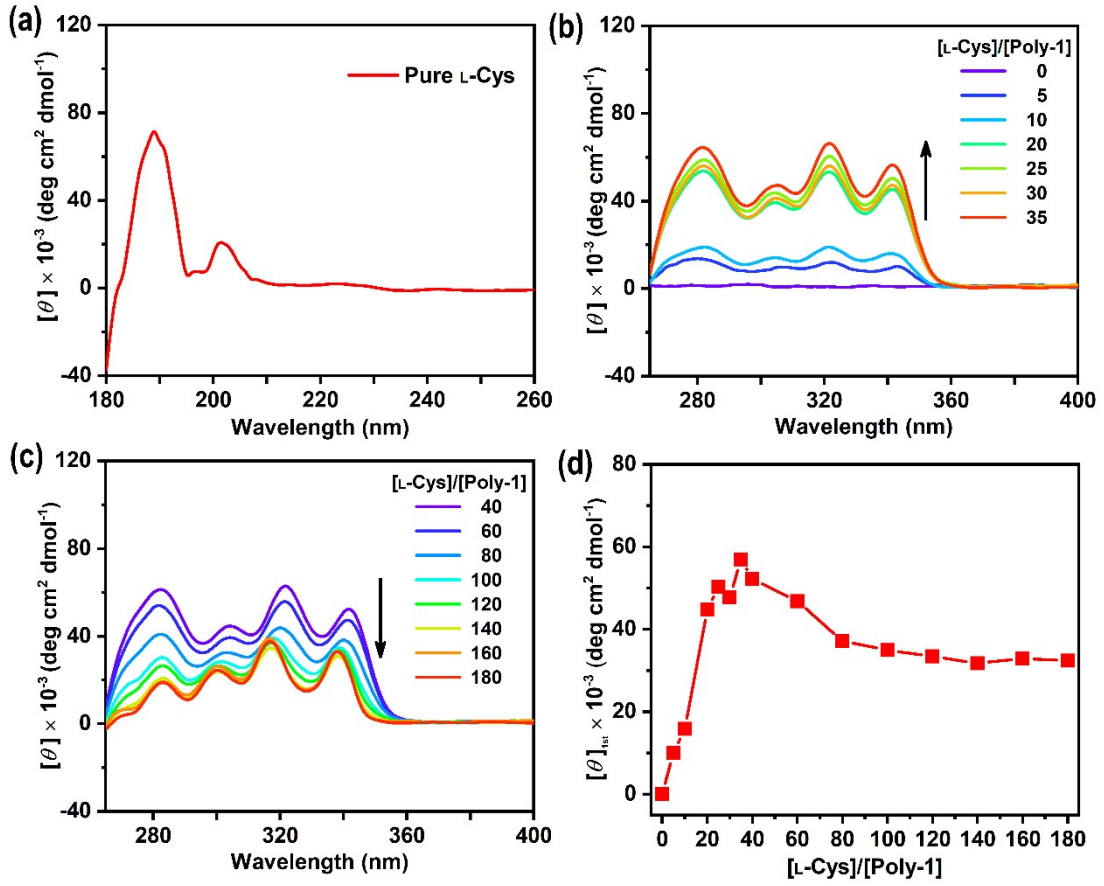

Fig. S16. CD spectra of pure L-**Cys** (a) and **Poly-1** in the presence of L-**Cys** (b, c) in $CHCl_3/CH_3CN$ (1/9, v/v) at room temperature. [**Poly-1**] = 240 μM. (d) Plot of CD intensity of the 1st Cotton effect for **Poly-1** versus the concentration ratio of L-**Cys** to **Poly-1**.

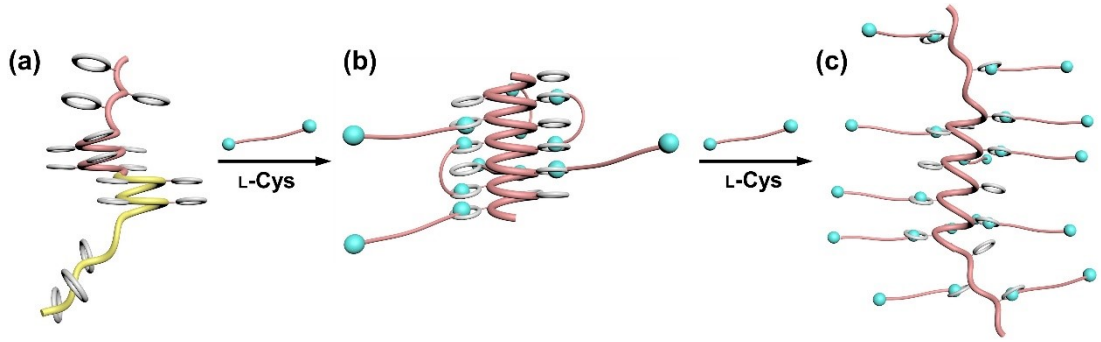

Scheme S2. Illustrative formation mechanism of chiral **Poly-1**/L-**Cys** complexes.

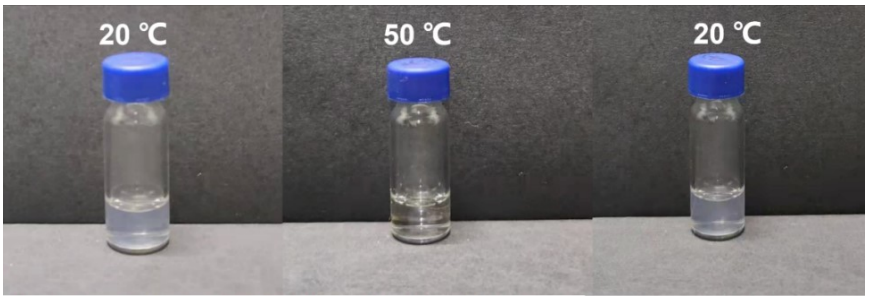

Fig. S17. Photographs of **Poly-1** in the presence of 40 equiv L-**Hcy** in $CHCl_3/CH_3CN$ (1/9, v/v) when heated from 20 to 50 °C and then cooled to 20 °C. [**Poly-1**] = 240 μM.

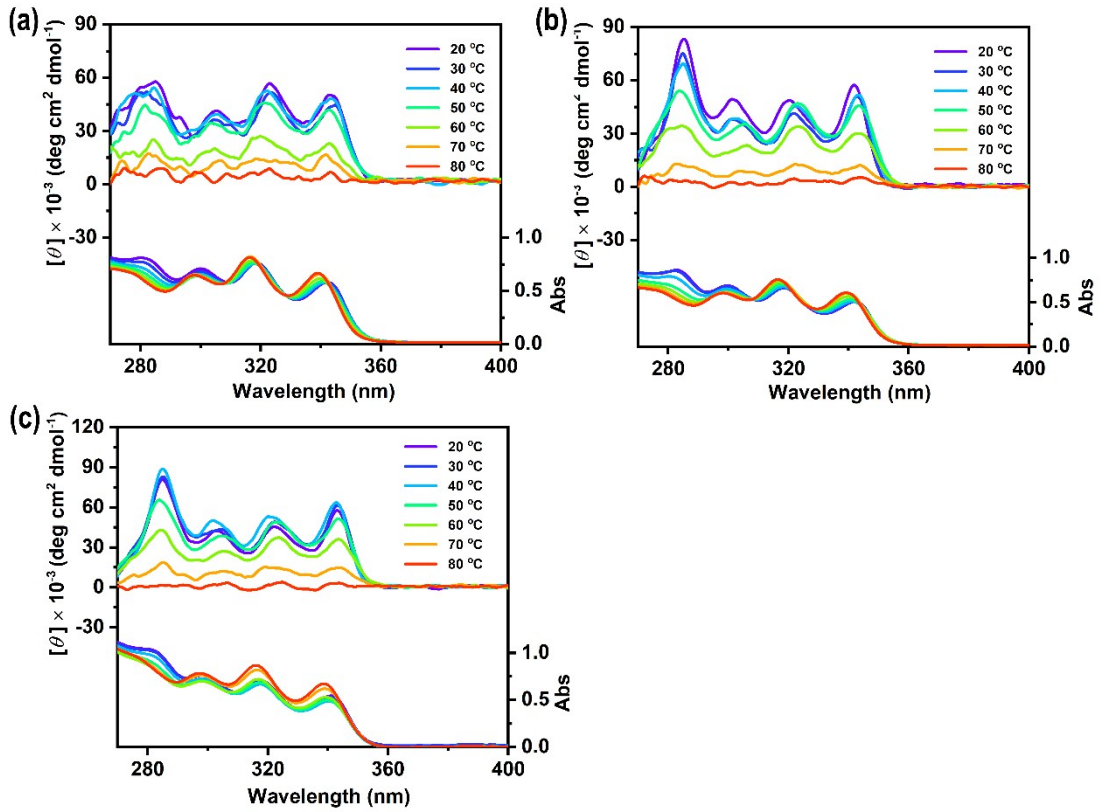

Fig. S18. CD (top) and UV–Vis absorption (bottom) spectra of **Poly-1** complexed with L-**Hcy** at a [L-**Hcy**]/[**Poly-1**] ratio of 5/1 (a), 10/1 (b) and 20/1 (c) in $CHCl_3/CH_3CN$ (1/9, v/v) at different temperature. [**Poly-1**] = 240 μM.

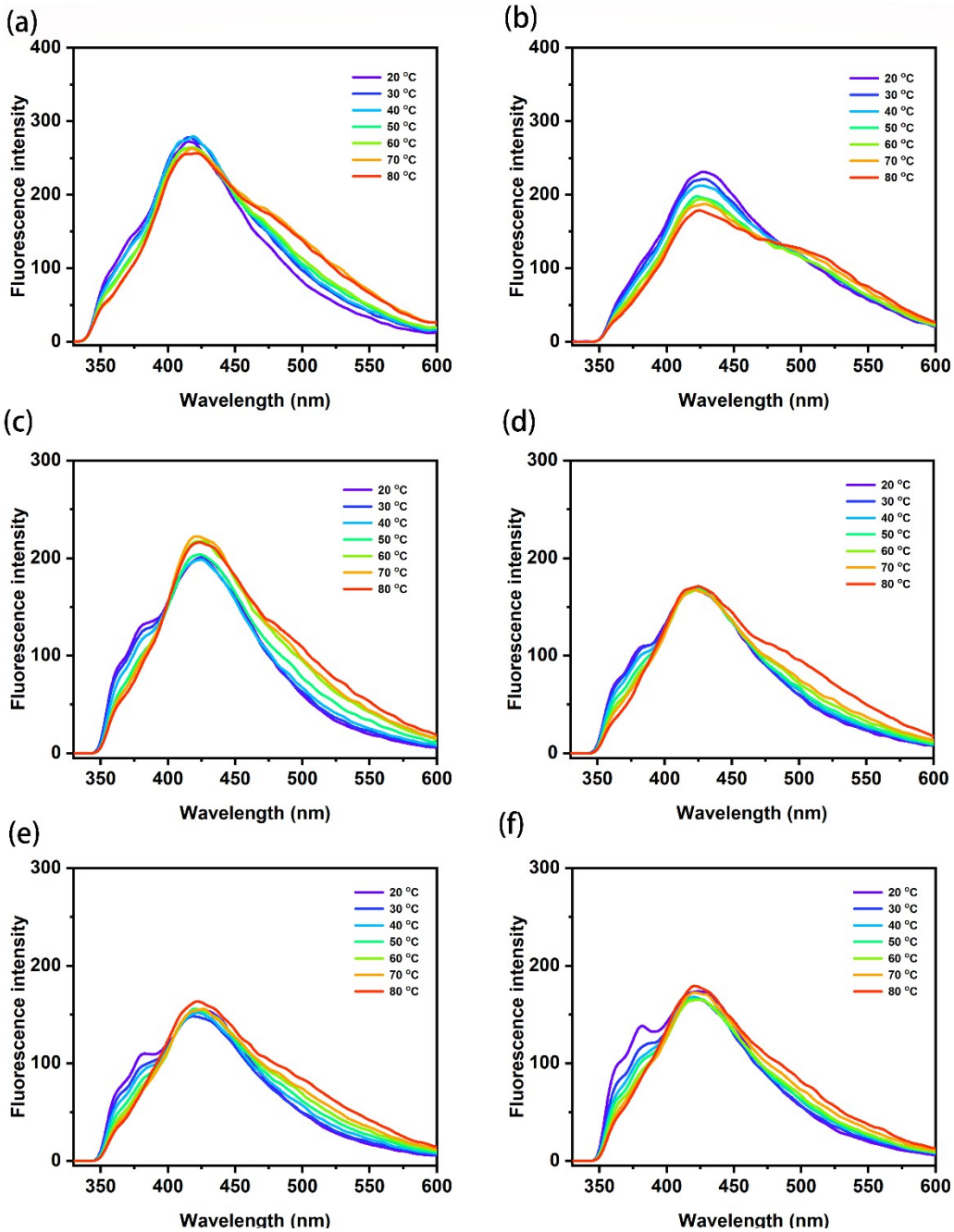

Fig. S19. Fluorescence spectra of **Poly-1** complexed with L-**Hcy** at a [L-**Hcy**]/[**Poly-1**] ratio of 5/1 (a), 10/1 (b), 20/1 (c) 25/1 (d), 30/1 (e) and 35/1 (f) in $CHCl_3/CH_3CN$ (1/9, v/v) at different temperature. [**Poly-1**] = 240 μM; λ_{ex} = 310 nm.

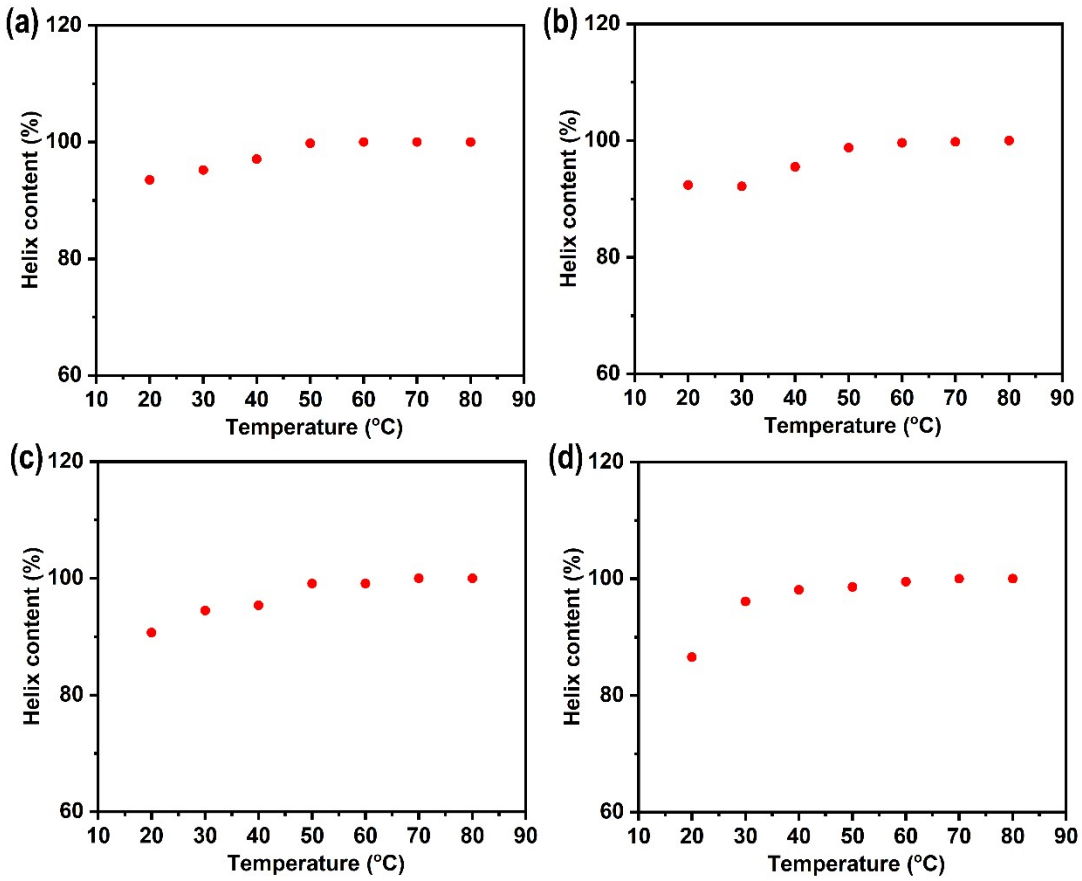

Fig. S20. Plots of helix content for **Poly-1** complexed with L-**Hcy** at a [L-**Hcy**]/[**Poly-1**] ratio of 20/1 (a) 25/1 (b), 30/1 (c) and 35/1 (d) versus temperature.

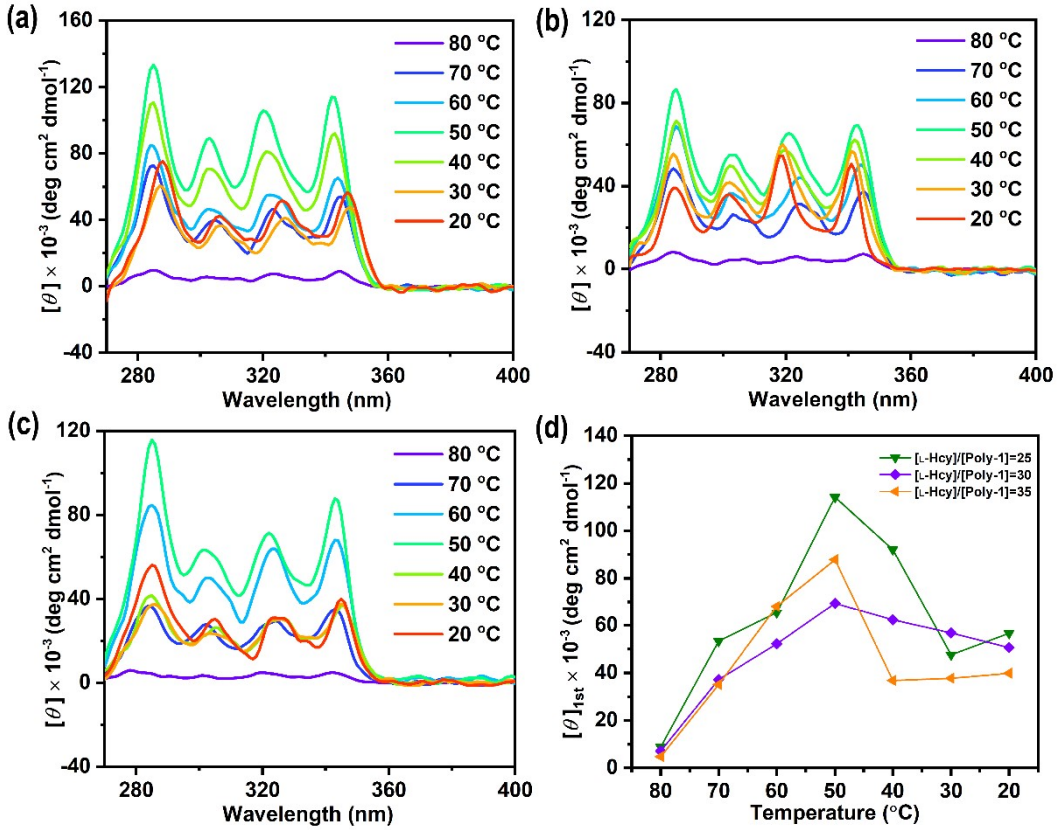

Fig. S21. CD spectral changes of **Poly-1** complexed with L-**Hcy** at a [L-**Hcy**]/[**Poly-1**] ratio of 25/1 (a), 30/1 (b) and 35/1 (c) in $CHCl_3/CH_3CN$ (1/9, v/v) during the cooling process. [**Poly-1**] = 240 μM. (d) Plots of CD intensity of the 1st Cotton effect for **Poly-1** with different content of L-**Hcy** versus the temperature.

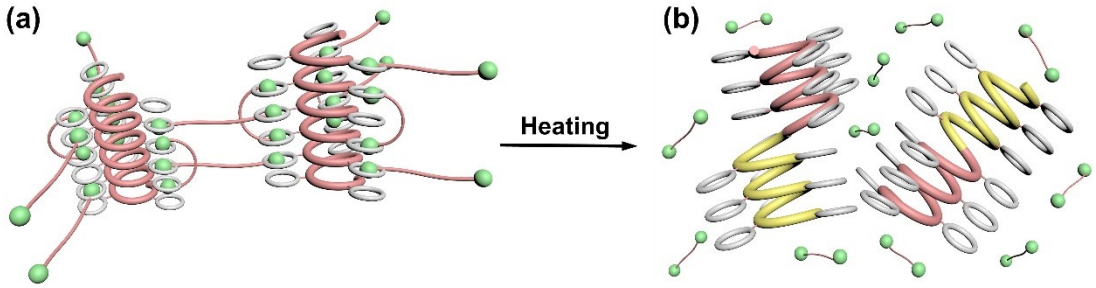

Scheme S3. Illustrative mechanism of thermotropic chirality decrease of **Poly-1**/L-**Hcy** nanoparticles at the [L-**Hcy**]/[**Poly-1**] ratios of 5/1 and 10/1.